1-Palmitoyl-2-pyrenedecanoyl Glycerophospholipids as Membrane Probes: Evidence for Regular Distribution in Liquid-Crystalline Phosphatidylcholine Bilayers†

Pentti J. Somerharju,*,‡ Jorma A. Virtanen,§ Kari K. Eklund,∥ Petri Vainio,∥ and Paavo K. J. Kinnunen∥
Departments of Basic Chemistry, Organic Chemistry, and Medical Chemistry, University of Helsinki, Helsinki, Finland
Received May 15, 1984

ABSTRACT: We have synthesized 1-palmitoyl-2-pyrenedecanoyl-*sn*-glycero derivatives of 3-phosphatidylcholine, 3-phosphatidylethanolamine, 3-phosphatidylserine, 3-phosphatidylglycerol, 3-phosphatidylinositol, and 3-phosphatidic acid and investigated their behavior in monolayers and in neat and mixed bilayers. Fluorescence spectroscopy of neat pyrene phospholipid dispersions revealed a well-defined thermotropic transition at 13.5–19 °C depending on the polar head group. An endotherm coinciding with this transition was observed with differential scanning calorimetry, indicating it to be due to the melting of the lipid acyl chains. For pyrenephosphatidylethanolamine, the endotherm was observed at a much higher temperature (70 °C). Compression isotherms obtained at an argon/water interface revealed that the pyrene moiety somewhat increases the mean molecular area of a phospholipid molecule but does not prevent the expression of head-group-dependent packing behavior. Partition of the pyrene lipids between coexisting fluid and solid phases was investigated with fluorometry and calorimetry. Both techniques indicate that these lipids prefer the fluid phase and that this preference is independent of the head group. The rates and apparent activation energies of lateral diffusion in fluid bilayers were found to be similar for most pyrene lipids, suggesting that the lateral movement of phospholipids is not critically dependent on interactions at the head-group level. Lateral distribution of the pyrene lipids in gel and fluid phosphatidylcholine bilayers was studied with the excimer technique and calorimetry. In gel-state dipalmitoylphosphatidylcholine bilayers, the pyrene lipids form clusters. These clusters, however, do not consist of pure pyrene lipid but of aggregates (compounds) of the labeled and unlabeled lipid. The stoichiometry of these aggregates seems to depend on the head group of the labeled lipid. In fluid bilayers, the pyrene lipids tend to adapt a regular rather than random or clustered distribution. This is suggested by the excimer to monomer intensity ratio vs. pyrene lipid mole fraction plots, which consist of several linear regions separated by kinks. The data for different pyrene lipids are alike, indicating that the lateral distribution of these lipids is governed by the pyrene moiety. The tendency of the pyrene lipids to distribute regularly is proposed to result from the presence of long-range order in liquid-crystalline bilayers.

The last few years have seen an exponential increase of membrane research employing fluorescent probes. The popularity of the fluorescence technique is due to its sensitivity as well as the relative simplicity of basic methodology and instrumentation. Furthermore, recent development of the theoretical aspects of fluorescence spectroscopy of membranes [for reviews, see Lakowitz (1981) and Yegurabide & Foster (1981)] allows one to obtain more detailed information than was possible before.

Most of the studies done so far have employed probes bearing little structural resemblance to the natural membrane constituents and which report on some bulk property of the membranes they have been incorporated into. An example is diphenylhexatriene, which is commonly used to monitor fluidity or "microviscosity" of the membrane hydrocarbon region (Shinitzky et al., 1971; Lentz et al., 1976). Although such probes have provided a lot of useful information on simple model systems, they are not very helpful when detailed information on the behavior of individual phospholipid molecules in complex mixtures such as natural membranes is required. Accordingly, several investigators have explored the use of phospholipid analogues containing a covalently coupled fluorescent moiety such as pyrene, anthracene, parinaric acid, and 4-nitro-2,1,3-benzoxadiazole. These analogues have been used to study a variety of membrane phenomena including lateral diffusion (Galla & Hartman, 1980), passive (Roseman & Thompson, 1980; Massey et al., 1982) and protein-mediated (Somerharju et al., 1981) transfer of phospholipids, intracellular translocation (Pagano et al., 1983) of phospholipids, lipid–protein interactions (Molotkovsky et al., 1982), membrane fusion (Struck et al., 1981), phospholipid phase transitions (Sklar et al., 1977; Galla & Hartmann, 1980), and the action of phospholipases A (Thuren et al., 1983, 1984).

Pyrene is a versatile lipid probe due to its spectroscopic properties. The emission spectra of pyrene and its derivatives typically show two components: one due to the excited pyrene monomers and the other, at longer wavelengths, originating from excimers formed upon collision of an excited pyrene with a ground-state pyrene. The ratio of excimer to monomer fluorescence intensities (I_e/I_m)[1] is proportional to the collision frequency of pyrenes, which in turn depends on the local concentration and diffusion rate of pyrene or its derivatives (Förster, 1969). Thus, I_e/I_m provides information on, for instance, phospholipid phase transitions and the rate of lateral diffusion and distribution of the labeled phospholipids in membranes (Galla & Hartman, 1980).

We have synthesized six glycerophospholipids containing

† This work was supported by a grant (to P.K.J.K.) from the Finnish State Medical Research Council.
‡ Department of Basic Chemistry.
§ Department of Organic Chemistry.
∥ Department of Medical Chemistry.

0006-2960/85/0424-2773$01.50/0

a pyrenedecanoyl chain in the *sn*-2 position and investigated their behavior in neat monolayers and in neat or mixed bilayers.

Materials and Methods

Lipids. Dipalmitoylphosphatidylcholine was a product of Sigma. 1-Palmitoyl-*sn*-glycero-3-phosphocholine was prepared from DPPC by phospholipase A_2 catalyzed hydrolysis and purified by acetone precipitation (Kates, 1972). Egg phosphatidylcholine was isolated according to Singleton et al. (1965). Phosphatidic acid was prepared by phospholipase D catalyzed hydrolysis of egg phosphatidylcholine (Davidson & Long, 1958). Yeast phosphatidylinositol was extracted from autolyzed bakers' yeast (Trevelyan, 1966) and purified as described earlier (Somerharju & Wirtz, 1982). Pyrenedecanoic acid was a product of KSV Chemicals (Valimotie 7, Helsinki, Finland). 1-Palmitoyl-2-pyrenedecanoyl-*sn*-glycerol-3-phosphate derivatives were prepared as follows: PyrPC was synthesized from 1-palmitoyl-*sn*-glycero-3-phosphocholine and pyrenedecanoyl anhydride (Gupta et al., 1977) and purified by silicic acid chromatography. PyrPE, -PS, -PG, and -PA were obtained by phospholipase D catalyzed transphosphatidylation or hydrolysis of PyrPC and were purified by preparative TLC on silicic acid plates (Merck) using either chloroform/methanol/NH_4OH/water (90:54:5.5:5.5 v/v) or chloroform/methanol/acetic acid/water (25:15:4:2 v/v) as solvent. PyrPI was synthesized from yeast phosphatidylinositol essentially as described before for the corresponding parinaroyl lipid (Somerharju & Wirtz, 1982). However, to improve the yield, the last stage of the synthesis, which involves the removal of the protecting acetyl groups from the inositol moiety, was carried out as follows. Peracetylated PyrPI (64 μmol) was dissolved in 260 μL of heptane, and 2.6 mL of water and 320 μL of hydrazine hydrate were added (all solvents were argon saturated). The two-phase mixture was stirred under argon for 2.5 h, and then 6 mL of chloroform, 3 mL of methanol, and 1 mL of 2% NaCl solution were added. After partition, the lower phase was washed first with 3 mL of methanol/0.1 M HCl (1:1 v/v) and subsequently with 3 mL of methanol/0.1 M NH_4OH (1:1 v/v). The final lower phase was taken to dryness and the residue dissolved in chloroform/methanol (9:1). The crude PyrPI was purified on a silicic acid column eluted with a graded series of chloroform/methanol mixtures. Thereafter, this lipid was subjected to reverse-phase high-pressure chromatography on a Waters C_{18} column using 20 mM choline chloride in methanol/water/acetonitrile (90.5:7:2.5 v/v) as eluent (Patton et al., 1982). Three major pyrene-containing peaks eluted. According to gas–liquid chromatographic analysis, the first of these consisted of the 1-palmitoleyl species (15% of total) and the second and third of palmitoyl (55%) and stearoyl (28%) species, respectively. In addition to pyrenedecanoic and palmitic acids, the second fraction contained about 2% oleic acid, which originates from the 1-oleyl-2-pyrenedecanoyl species not completely resolved from the corresponding 1-palmitoyl lipid. The total yield of purified PyrPI molecular species was 10.3 μmol.

All lipids were analyzed by TLC and were >98% pure. To estimate the acyl chain purity of pyrene phospholipids, the molar absorption coefficient was calculated from the phosphorus content and pyrene absorbance of PyrPI consisting of a single molecular species (see above). A value of 42 000 $M^{-1}\cdot cm^{-1}$ was obtained for ϵ_{342} in ethanol. On the basis of this value and phosphorus analysis (Rouser et al., 1967), the pyrene content of PyrPC, -PE, -PS, -PG, -PI, and -PA was calculated to be 1.0, 0.87, 0.90, 0.89, 1.0, and 0.94, respectively. The lower pyrene to phosphorus ratio observed for some of the lipids could be due to dilution of the pyrene derivative by unlabeled species originating from the phospholipase D preparation used in their synthesis. Alternatively, some breakdown or chemical modification of the pyrene moiety may have taken place during their synthesis. However, UV spectra of all the lipids were identical, which argues against the latter alternative.

Preparation of Liposomes. Multilamellar liposomes were prepared according to conventional methods. Lipids dissolved in chloroform/methanol were taken to dryness (finally from chloroform) under a stream of nitrogen and evacuated subsequently for several hours. The dry lipids were then dispersed in an argon-saturated buffer by vortexing or by brief sonication (5–10 s) under an argon atmosphere at 45 °C using a Branson sonicator equipped with a microtip and operated at 40-W output.

Fluorescence Measurements. All fluorescence measurements were carried out with an SLM 4800 instrument equipped with a thermostated cuvette holder and connected to a Hewlett-Packard 85 computer. All spectra are uncorrected. The excimer (475 nm) to monomer (377 nm) intensity ratios (I_e/I_m) were calculated from the computer printout of the spectral data. At the selected wavelengths, the contribution of the monomer to the excimer fluorescence, and vice versa, is negligible (less than 1.5%) and thus warrants no correction. Some inner filtering occurs at the higher pyrene lipid concentrations, but this reduces monomer and excimer intensities in the same proportion and thus does not influence I_e/I_m. The outer filtering effect is of concern in the case of monomer fluorescence, since the pyrene residues absorb slightly (ϵ_{377} = 800 $M^{-1}\cdot cm^{-1}$) at the corresponding wavelength. However, even at the highest pyrene phospholipid concentrations used (7×10^{-6} M), the absorbance at 377 nm was below 0.01, and thus the outer filtering effect can be safely neglected.

In temperature scans, I_e/I_m was recorded directly by using the two-channel detection system of the SLM instrument. The monomer peak at 377 nm was isolated with a monochromator and the excimer peak with a 450-nm cutoff filter. Excitation was at 343 nm. Before excitation, the samples were incubated at 4 °C for 20 min. The scanning rate was approximately 1.4 °C/min. Some scans were also carried out at a heating rate of 0.5 °C/min.

Fluorescence lifetimes were determined with the demodulation method (Spencer & Weber, 1970). The excitation polarizer was set to an angle of 35° in order to eliminate the influence of Brownian motion on the measured lifetimes (Spencer & Weber, 1970). POPOP was used as the lifetime reference (Lakowicz et al., 1981). Samples were kept under an argon atmosphere during measurement.

[1] Abbreviations: PyrPC, 1-palmitoyl-2-pyrenedecanoyl-*sn*-glycero-3-phosphocholine; PyrPE, 1-palmitoyl-2-pyrenedecanoyl-*sn*-glycero-3-phosphoethanolamine; PyrPS, 1-palmitoyl-2-pyrenedecanoyl-*sn*-glycero-3-phosphoserine; PyrPI, 1-palmitoyl-2-pyrenedecanoyl-*sn*-glycero-3-phospho-*myo*-1-inositol; PyrPG, 1-palmitoyl-2-pyrenedecanoyl-*sn*-glycero-3-phospho-*rac*-1(3)-glycerol; PyrPA, 1-palmitoyl-2-*sn*-glycerol 3-phosphate; PD, pyrenedecanoyl; DPPC, 1,2-dipalmitoyl-*sn*-glycero-3-phosphocholine; EPC, 1,2-diacyl-*sn*-glycero-3-phosphocholine from egg yolk; NaEDTA, sodium salt of ethylenediaminetetraacetic acid; Tris, tris(hydroxymethyl)aminomethane; POPOP, 1,4-bis[2-(5-phenyloxazolyl)]benzene; T_m, transition temperature; ΔE, apparent activation energy; HSDSC, high-sensitivity differential scanning calorimetry; I_e/I_m, ratio of excimer to monomer fluorescence intensities; X_{PyrPL}, mole fraction of the indicated pyrene phospholipid; TLC, thin-layer chromatography; EPR, electron paramagnetic resonance; Tempo, 2,2,6,6-tetramethylpiperidinyl-1-oxy.

Determination of Activation Energies for Lateral Diffusion of Pyrene Phospholipids in EPC and DPPC. Following Galla & Hartman (1980), we calculated the relative values of the lateral diffusion constants (D_{rel}) for pyrene lipids from

$$D_{rel} = k\frac{I_e}{I_m}\frac{1}{\tau_e} \quad (1)$$

where I_e and I_m are the excimer and monomer fluorescence intensities, respectively, τ_e is the fluorescence lifetime of the excimer, and k is a combined term, which is independent of temperature and can thus be neglected. Accordingly, calculation of the apparent activation energies requires only the knowledge of I_e/I_m and τ_e as a function of temperature. τ_e was measured for each pyrene lipid in EPC (1:9 mole ratio) and was found to be practically independent of the head group. In the DPPC bilayer, the lifetimes were measured for PyrPC only and were used to calculate D_{rel} also for the other pyrene lipids. In EPC, τ_e decreased linearly from 114 ± 15 ns at 27 °C to 81 ± 10 ns at 42 °C, and in DPPC from 78 ns at 43 °C to 61 ns at 55 °C. Also, the log D_{rel} vs. $1/T$ plots were essentially linear in all cases.

Differential Scanning Calorimetry. Differential heat capacity measurements were carried out with a Privalov DASM-1M instrument equipped with an X–Y recorder. The scanning rate was 1 °C/min. Samples were equilibrated in the cuvette at 4 °C for at least 0.5 h before the scan was started.

Molecular Surface Area Measurements. Compression isotherms were obtained with a KSV 2200 surface barostat (KSV Chemicals Oy, Helsinki, Finland) equipped with a rectangular Teflon trough (169 × 280 mm). The subphase was 20 mM Tris-HCl, 100 mM NaCl, and 1 mM NaEDTA, pH 7.4, prepared in doubly distilled water. The lipids were applied in chloroform/methanol, and compression was started after a 3-min equilibration period. Surface pressure was measured with the Wilhelmy plate method. The isotherms for pyrene phospholipids were obtained under an argon atmosphere and were completely reversible.

Results and Discussion

Thermotropic Behavior of Neat Pyrene Phospholipid Dispersions. Since all of the pyrene lipids were not available in quantities sufficient for calorimetry, we applied a fluorometric technique to obtain the T_m of these lipids. This is based on the finding that in aqueous dispersions of neat pyrene phospholipids I_e/I_m is strongly temperature dependent (Figure 1). I_e/I_m vs. temperature scans for PyrPC, -PS, -PG, and -PI display a marked, abrupt increase in I_e/I_m centered at 14.0, 13.5, 16.0, and 19.0 °C, respectively (Figure 2). HSDSC showed an endothermic transition for PyrPC (Figure 6) and PyrPG (not shown) dispersions at 15 and 17 °C, respectively. These values are close to those obtained by the fluorometric procedure, indicating that the latter is monitoring the gel to liquid-crystalline phase transition. It is relevant to note that major changes take place in the EPR spectrum of neat spin-labeled phosphatidylcholine dispersions at the main transition (Chen & Gaffney, 1978; Chen et al., 1982).

Considerable hysteresis seems to be associated with the phase transition of neat pyrene phospholipid bilayers. For instance, the cooling curve of PyrPI was shifted down by several degrees centigrade in the transition region as compared to the heating curve (not shown).

The reason for the decreased I_e/I_m of the pyrene lipids in the gel state is not clear but could be due to tilting of the acyl chains. Such tilting, which is necessary in order to accommodate the polar head groups (Hauser et al., 1981), could

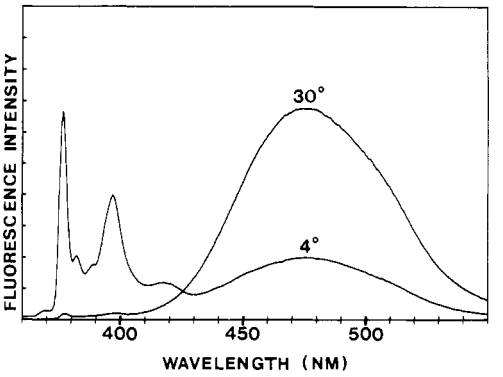

FIGURE 1: Emission spectra for neat PyrPI liposomes at 4 and 30 °C. Excitation was at 343 nm, slit 2 nm. The buffer was 20 mM Tris-HCl, 100 mM NaCl, and 1 mM NaEDTA, pH 7.4. The samples were equilibrated for 20 min at the indicated temperatures before recording was started. The spectra have been normalized to the same peak intensity.

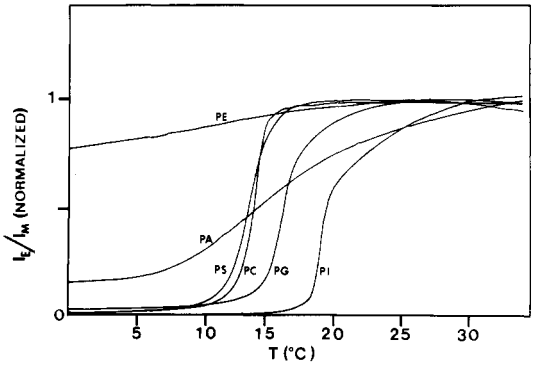

FIGURE 2: Fluorometrically detectable thermotropic phase transitions in pyrene phospholipid dispersions. I_e/I_m was recorded continuously vs. increasing temperature for dispersions of pure pyrene phospholipids prepared by suspending the dried lipids into 20 mM Tris-HCl, 100 mM NaCl, and 1 mM NaEDTA, pH 7.4, using a 5-s sonication pulse at 40 °C. For other details, see Materials and Methods.

hamper juxtaposition of the pyrene moieties and thus decrease I_e/I_m. The involvement of tilt is supported by two pieces of data. First, we have found that the addition of Ca^{2+} ions into dispersions of acidic phospholipids largely prevents the decrease of I_e/I_m upon cooling to 4 °C (unpublished results). Binding of Ca^{2+} obviously condenses the head-group region which makes tilting unnecessary. Second, below T_m, I_e/I_m is much higher for PyrPA than for other acidic pyrene lipids and PyrPC (Figure 2). It is known that close to neutral pH phosphatidic acid in neat bilayers bears only one negative charge and is capable of forming intermolecular hydrogen bonds (Boggs, 1980), which reduces the effective size of the head group. Thus, less tilt is required in the gel-state phosphatidic acid bilayers.

In contrast to other pyrene lipids, a clear transition was not observed for PyrPE by the fluorometric technique in the temperature range studied (Figure 2). HSDSC revealed an endothermic transition (data not shown), but this occurred at such a high temperature (70 °C) that it probably is not due to the normal gel to liquid phase transition. More likely, this transition corresponds to the simultaneous hydration and acyl chain melting transition previously observed in dispersions of saturated phosphatidylethanolamines (Mantsch et al., 1983; Chang & Epand, 1983). PyrPE, unlike other pyrene lipids, could be dispersed in buffer only with difficulty. In addition, the emission spectrum of PyrPE dispersions displayed a short-wavelength shoulder on the excimer peak (not shown) which was absent from the spectra of other pyrene lipids. These findings further indicate that the physical state of PyrPE

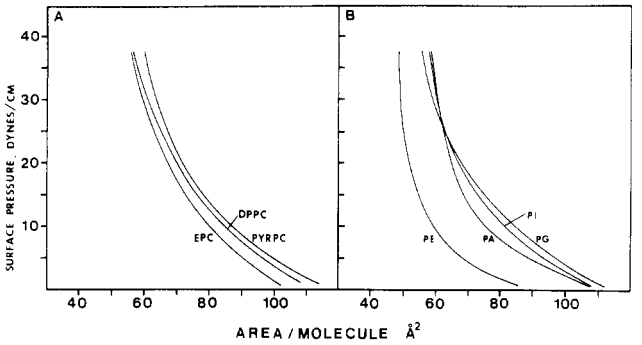

FIGURE 3: Surface isotherms for (A) PyrPC, EPC, and DPPC and for (B) PyrPE, -PA, -PG, and -PI. The subphase consisted of 20 mM Tris-HCl, 100 mM NaCl, and 1 mM NaEDTA, pH 7.4. The temperature was 48 ± 1 °C for DPPC and 37 ● 1 °C for other lipids. The abbreviations PE, PA, PG, and PI refer to the corresponding pyrene lipids.

Table I: Molecular Surface Areas for Pyrene Phospholipids, DPPC, and EPC at a Surface Pressure of 35 dyn/cm[a]

lipid	area/molecule (Å²)	lipid	area/molecule (Å²)
DPPC	58	PyrPG	57
EPC	57	PyrPI	59
PyrPC	61	PyrPA	59
PyrPE	49		

[a] The subphase was 20 mM Tris-HCl, 100 mM NaCl, and 1 mM NaEDTA, pH 7.4, and the temperature was 48 ± 1 °C for DPPC and 37 ● 1 °C for other lipids. Each value is a mean of three independent determinations. The surface area of PyrPS could not be determined due to the small amount of material available.

is different from that of the other pyrene lipids. Poor hydration of PyrPE and some other ethanolamine phospholipids is obviously due to the absence of a repulsive net charge and their ability to form intermolecular hydrogen bonds [see Hauser et al. (1981) and Boggs (1980)].

Properties of Neat Pyrene Phospholipid Monolayers. Properties of pyrene phospholipids were further investigated by recording the compression isotherms for neat pyrene phospholipid monolayers spread on an argon/water interphase at 37 °C. For comparison, isotherms were recorded also for DPPC (at 48 °C) and EPC (Figure 3). The isotherms of PyrPC, EPC, and DPPC are quite similar which indicates that the pyrene moiety does not appreciably influence the packing properties. The surface area occupied by the pyrene derivative appears, however, to be somewhat larger than that of the alkyl chain lipids (Table I). The absence of transitions suggests, in accordance with the data on thermotropic behavior discussed above, that the T_m of PyrPC is well below the experimental temperature, i.e., 37 °C. The isotherms of PyrPI and -PG resemble closely that observed for PyrPC although the effective surface areas of these lipids seem to be somewhat smaller (Table I). The isotherm of PyrPA is different from those of PyrPC, -PI, and -PG in that it rises more steeply at higher surface pressures. This is probably due to repulsive Coulombic forces which become effective at closer packing of the PyrPA molecules.

PyrPE forms more condensed monolayers than the other pyrene lipids (Figure 3B and Table I). This behavior has been found also for alkyl chain phosphatidylethanolamines (van Deenen et al., 1962) and can be attributed to the ability of ethanolamine lipids to form intermolecular hydrogen bonds as well as to the absence of a repulsive net charge.

In conclusion, it appears that although the pyrene moiety seems to slightly increase the effective surface area of a phospholipid, it does not dominate the packing properties of the lipid, at least to the extent that specific interactions at the head-group level would be masked.

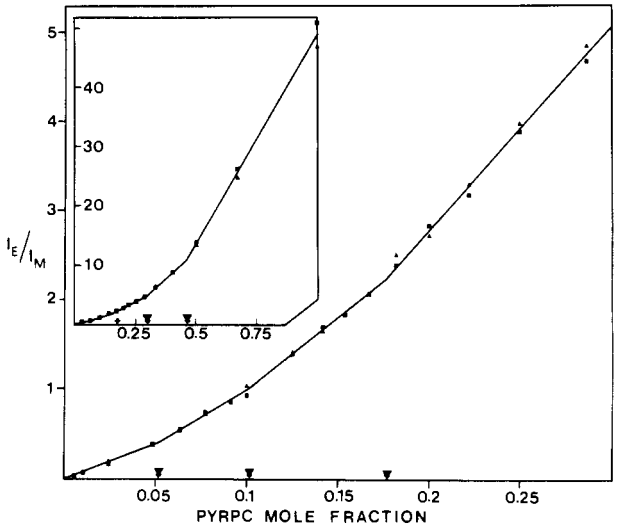

FIGURE 4: Ratio of excimer to monomer fluorescence intensities vs. X_{PyrPC} in PyrPC/EPC mixtures. Liposomes containing the indicated amounts of PyrPC in EPC were prepared, and I_e/I_m was determined from the emission spectra as explained under Materials and Methods. The buffer was 20 mM Tris-HCl, 100 mM NaCl, and 1 mM Na-EDTA, pH 7.4. Excitation was at 343 nm, slit 2 nm; the emission slit was 4 nm. Data are from two independent experiments (▲, ■). In the insert, I_e/I_m is plotted over the whole X_{PyrPC} range; some points have been omitted at low PyrPC mole fractions for clarity.

Table II: Observed Critical Pyrene Phospholipid Mole Fractions in EPC and DPPC[a]

pyrene lipid	matrix lipid	first kink	second kink	third kink	fourth kink	fifth kink
PyrPC	DPPC	3.8	6.8			
	EPC	5.0	10.0	17.7	30.0	46.0
PyrPE	DPPC	3.4	8.4			
	EPC	3.6	7.9			
PyrPS	DPPC	3.6	9.1			
	EPC	3.6	7.5			
PyrPG	DPPC	4.1	9.1			
	EPC	3.4	9.1			
PyrPI	DPPC	3.8	10.7			
	EPC	4.8	9.1			
PyrPA	DPPC	6.3				
	EPC	6.3				

[a] Based on the data given in Figures 4 and 5.

Lateral Distribution of Pyrene Phospholipids in the Liquid-Crystalline Phosphatidylcholine Matrix. There is little conclusive data available on the lateral distribution of phospholipids in liquid-crystalline, mixed bilayers (Boggs, 1980). Three principal modes of distribution can be distinguished: (i) separation into pure phases; (ii) regular distribution; and (iii) random (ideal) mixing of the components. In practice, intermediate cases may prevail over these extremes.

The distribution of pyrene lipids in phosphatidylcholine (EPC and DPPC) bilayers was determined by measuring I_e/I_m vs. X_{PyrPL}. The experimental temperature was chosen so that both the pyrene-labeled and the unlabeled (matrix) lipid would be in the liquid-crystalline state.

Figure 4 shows the plot of I_e/I_m vs. X_{PyrPC} in EPC at 37 °C. As expected, I_e/I_m increases first linearly and then progressively at higher PyrPC concentrations. Interestingly, however, the plot, rather than being smooth, consists of several close to linear regions separated by kinks. For the other pyrene lipid/EPC (DPPC) mixtures, a similar behavior was found (Figure 5). In general, the X_{PyrPL} values corresponding to the kinks as well as the slopes of the apparently linear regions are similar for most pyrene lipids (Tables II and III), suggesting

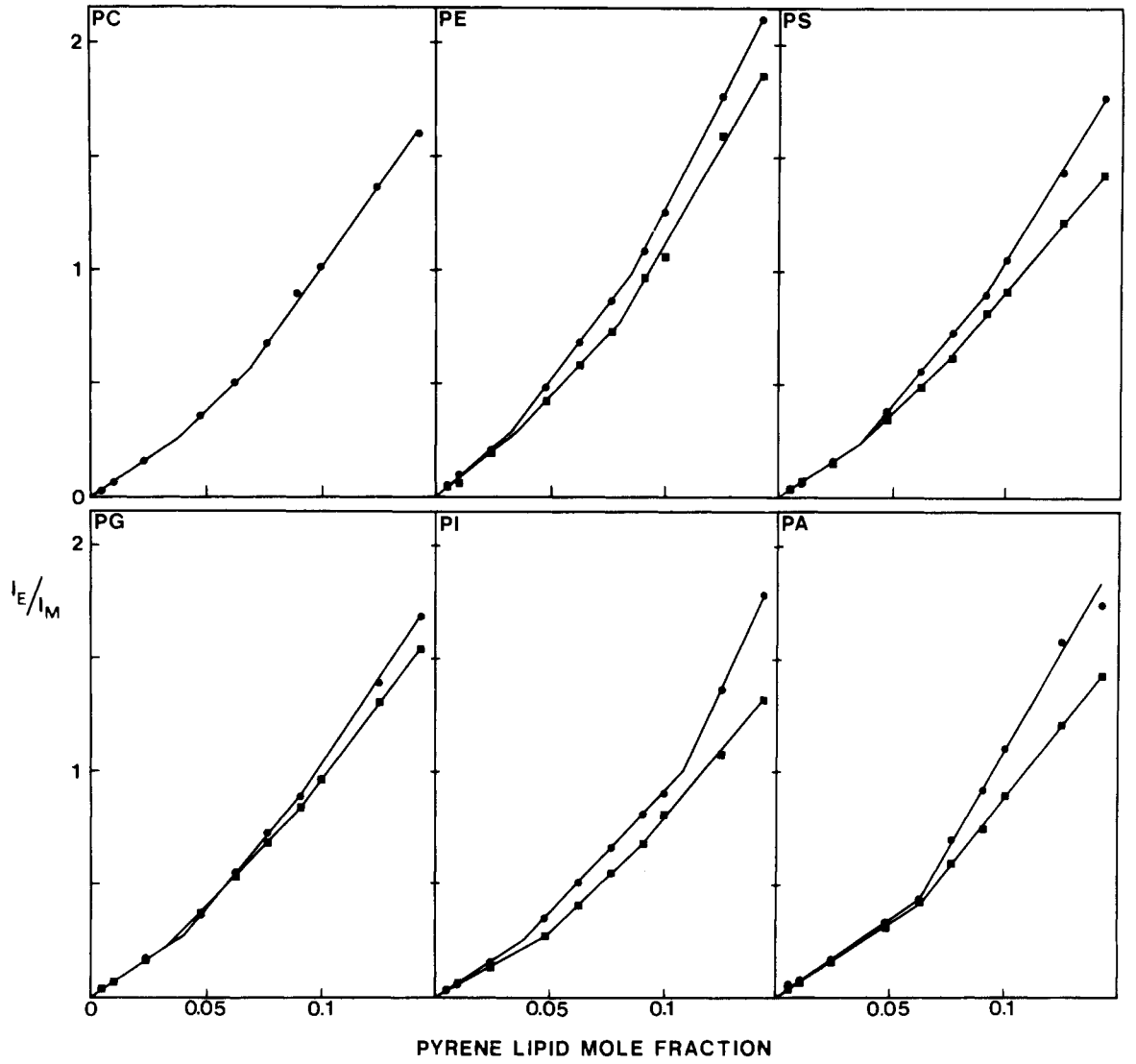

FIGURE 5: Ratio of excimer to monomer fluorescence intensities vs. X_{PyrPL} in EPC at 37 °C (■) and in DPPC at 48 °C (●). For other details, see the legend of Figure 4.

Table III: Slopes of I_e/I_m vs. Pyrene Phospholipid Mole Fraction Plots[a]

pyrene lipid	matrix lipid	slope 1	r^2	n	slope 2	r^2	n	slope 3	r^2	n
PyrPC	DPPC	6.72	1.000	3	10.0		2	14.0	0.999	5
	EPC	8.15	0.997	8	11.7	0.968	8	15.0	0.993	7
PyrPE	DPPC	7.73	0.994	3	13.4	1.000	3	19.8	1.000	4
	EPC	7.74		2	10.7	1.000	3	17.9	0.992	4
PyrPS	DPPC	6.50	0.998	3	12.1	1.000	4	16.7	0.998	4
	EPC	5.59	1.000	3	9.31	1.000	3	12.3	0.999	5
PyrPG	DPPC	6.99	1.000	3	12.3	0.999	4	15.8	0.995	4
	EPC	6.26	0.999	3	10.7	1.000	4	13.6	1.000	4
PyrPI	DPPC	6.25	0.979	3	10.6	0.999	5	22.8		2
	EPC	5.29	0.994	4	9.61	0.999	4	12.0	0.998	4
PyrPA	DPPC	6.61	0.999	5	16.8	0.990	6			
	EPC	6.52	0.997	5	12.8	0.999	6			

[a] The slopes and the corresponding correlation factors (r^2) have been obtained by the method of least squares. n = number of data points. The experimental temperature was either 37 °C (EPC) or 48 °C (DPPC).

that the mode of distribution is largely head group independent. Also, PyrPL distribution seems to be rather insensitive to the degree of saturation of the matrix lipid alkyl chains, since the critical mole fractions are similar in EPC and DPPC matrixes (Table II). The fact that the slopes tend to be somewhat higher for the DPPC matrix as compared to EPC (Table III) is probably due to the higher temperature (48 vs. 37 °C for EPC) used in these experiments.

The correlation coefficients (r^2) of the least-squares analysis of the apparently linear regions of the I_e/I_m vs. X_{PyrPL} plots were in most cases close or equal to unity (Table III), supporting the presence of discontinuities.

The I_e/I_m vs. X_{PyrPL} data suggest that the pyrene lipid molecules are not randomly distributed in the phosphatidylcholine matrix, since on the basis of theoretical studies (von Dreele, 1978) one would expect these plots to be smooth (i.e., to contain no kinks) if the lipids were randomly distributed. The possibility that phase separation or clustering would be responsible for the kinks in the I_e/I_m vs. X_{PyrPL} plots is made unlikely by the fact that the critical mole fractions appear to

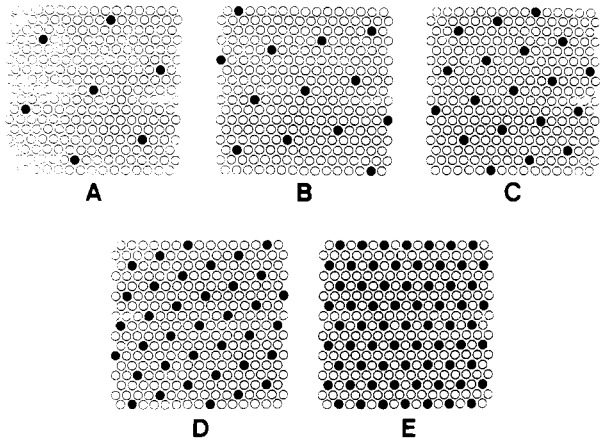

FIGURE 6: Hypothetical mean distributions of PD chains (closed circles) in an alkyl chain (open circles) lattice. The different patterns correspond to the critical PyrPC mole fractions (kinks) observed for PyrPC/EPC bilayers (Figure 4). The mole fractions, as predicted by the regular distribution model, are 0.054 (A), 0.095 (B), 0.154 (C), 0.0286 (D), and 0.500 (E). See text for other details.

be largely independent of the pyrene lipid head group (Table II). Due to lack of Coulombic repulsion, one would expect clustering of neutral (zwitterionic) PyrPC and -PE molecules to occur at lower mole fractions than that of charged PyrPI, -PS, and -PG molecules. In support of this, the critical mole fractions as well as the overall shape of the I_e/I_m vs. X_{PyrPL} plots are strongly head group dependent in crystalline DPPC where partial clustering of the pyrene lipids is obviously taking place (see below).

The fluorescence data can be readily explained in terms of a regular distribution model[2] based on the following assumptions: (i) the alkyl chains of the phospholipids form a hexagonal host lattice; (ii) PD chains represent quest elements, which cause steric perturbation in the host lattice; and (iii) the quest elements tend to be maximally separated in order to minimize the total free energy.

These basic assumptions have two important consequences: First, maximal (and equal) separation between the quest elements (PD chains) in a hexagonal host lattice is achieved when the quest elements establish a hexagonal superlattice within the host lattice (Figure 6). Second, the mean distance between quest elements is not a smooth function of the quest element mole fraction but obtains discrete values corresponding to the number of lattice sites separating proximal quest elements. In effect, this means that I_e/I_m, which depends on the average distance between PD chains, is also not a smooth function of X_{PyrPL}.

At low mole fractions, PD chains (quest elements) are probably more or less randomly distributed in the bilayer. The first kink (with increasing X_{PyrPL}) apparently corresponds to a situation where the regular distribution pattern of pyrene lipids first becomes observable over the whole bilayer (Figure 6, pattern A). When X_{PyrPL} further increases, this pattern is gradually converted to a new one (pattern B), where the inter-pyrene distance is necessarily shorter than that in the parent pattern. Thus, there will be an increase in the slope of the I_e/I_m vs. X_{PyrPL} plot at this point. We assume that the new, denser pattern does not mix with the parent pattern but forms a separate phase. Growth of the new phase continues until the next critical mole fraction is reached. At this point, the first pattern has been completely converted to the second one, and formation of a third, still denser pattern (C) ensues and so on. Thus, at each critical mole fraction, only a single phase characterized by a specific pyrene chain distribution pattern exists, while between two subsequent critical mole fractions two phases with different patterns coexist.[3]

It is stressed that the distribution patterns as described in Figure 6 are not implied as static but represent the mean, energetically most favorable distribution of the components.

We assume that the regular distribution of the pyrene lipids is due to the presence of the bulky, perturbing pyrene moiety, which induces steric elastic strain in the alkyl chain lattice [see Sackmann (1983)]; interactions in the head-group level are considered unimportant in this respect. However, some pyrene lipid head-group-dependent as well as matrix lipid dependent variations in the critical mole fractions are observed (Table II). For instance, the values of the first critical mole fraction for PyrPA is almost twice that observed for most of the other pyrene lipids. A feasible explanation for this is that the liposomes containing PyrPA are smaller than those containing other pyrene lipids. Membranes containing phosphatidic acid have a higher surface charge density than those containing equal amounts of neutral or singly charged lipids (Hauser & Dawson, 1967; Hauser et al., 1979) and are thus expected to disperse more readily and form smaller liposomes. Smaller size results in higher bilayer curvature, which causes distortion in chain packing (Horwitz et al., 1973; Lichtenberg et al., 1975; Petersen & Chan, 1977) and thus weakens the lattice forces responsible for the regular distribution of the pyrene lipid molecules. The other observed pyrene lipid head-group-dependent and matrix lipid dependent variations of the critical mole fractions (Table II) could be similarly attributed to differences in the size of the liposomes. Supporting this, we have observed that when small vesicles prepared by the ethanol injection method (Batzri & Korn, 1973) are used, the first kink is shifted to higher X_{PyrPL} values as compared to the larger liposomes used in this study (P. J. Somerharju, J. A. Virtanen, and P. K. J. Kinnunen, unpublished results).

The observed regular distribution of pyrene lipids in liquid-crystalline bilayers has many implications. Most importantly, it suggests that a lattice order of considerable range can exist also in the liquid-crystalline state. Such an order should have a strong influence on the lateral distribution of lipids, proteins, and other membrane-associated molecules (Sackmann, 1983).

Berclaz & McConnell (1981) have observed that partition of the Tempo spin-label into fluid dimyristoylphosphatidylcholine/cardiolipin bilayers shows several strong, composition-dependent discontinuities, from which they concluded that long-range, crystallike lateral order could be present in these bilayers. In this case, however, the order would result from repulsive Coulombic forces between the cardiolipin head groups and/or the counterions rather than from perturbation in the hydrocarbon region as in the case of the pyrene lipids.

Distribution of Pyrene Phospholipids in Gel-State DPPC. To study the interactions of pyrene phospholipids with alkyl chain phospholipids in the gel state, we investigated the phase transition properties of PyrPC/DPPC mixtures with HSDSC (Figure 7). Addition of only a few percent of PyrPC abolishes the pretransition of DPPC. The main transition is broadened and shifted to lower temperatures. A further increase of X_{PyrPC} leads to further broadening and a decrease in T_m until above

[2] J. A. Virtanen, P. J. Somerharju, and P. K. J. Kinnunen, manuscript in preparation.

[3] Preliminary theoretical considerations indicate that the appearance of kinks in the I_e/I_m vs. X_{PyrPL} plots does not require a regular arrangement of all the pyrene chains but a considerable fraction of them can be randomly distributed.

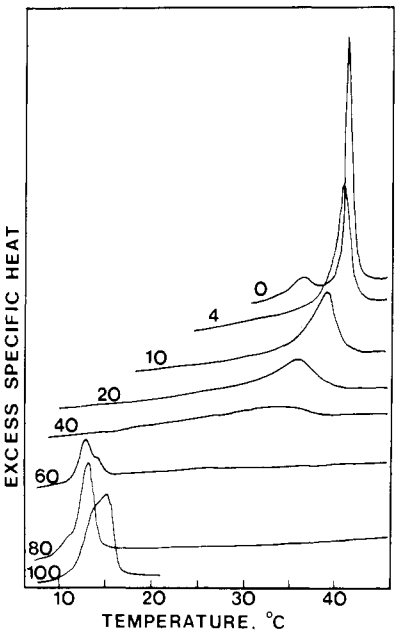

FIGURE 7: HSDSC heating scans for mixtures of PyrPC and DPPC. Multilamellar vesicles were prepared by dispersing the lipids in 20 mM Tris-HCl, 100 mM NaCl, and 1 mM NaEDTA, pH 7.4, by vortexing at approximately 50 °C. The samples were equilibrated for several hours at 4 °C before scanning. Lipid concentration was 1 mg/mL and sample volume 1 mL. Scan rate was 1 °C/min.

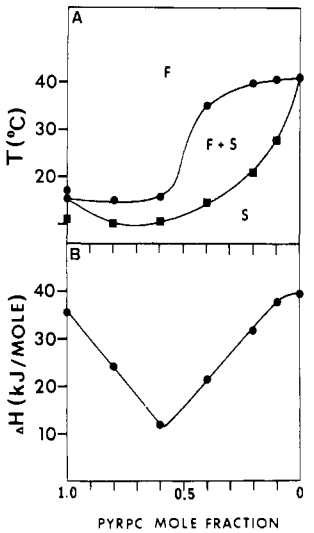

FIGURE 8: Thermotropic behavior of PyrPC/DPPC mixtures. (A) Phase diagram for PyrPC/DPPC constructed on the basis of the calorimetric data presented in Figure 7. Transition onset (■) and completion (●) temperatures were used to obtain the solidus and fluidus curves, respectively. S, solid phase; F, fluid phase. (B) Phase transition enthalpy for PyrPC/DPPC mixtures vs. X_{PyrPC}. Enthalpies were calculated from the transition curves given in Figure 7.

60 mol % the transition starts becoming sharper again. A phase diagram for PyrPC/DPPC constructed on the basis of the calorimetric data is shown in Figure 8A. Clearly, the mixing of the lipids is not ideal. Yet, monotectic behavior (coexistence of pure component phases) is not observed. The solidus and possibly also the fluidus lines display a minimum close to $X_{PyrPC} = 0.3$, suggesting formation of stoichiometric aggregates (compounds) (van Dijck et al., 1977; Sturtevant et al., 1979).

The transition enthalpies of PyrPC/DPPC mixtures are plotted in Figure 8B. While the transition enthalpy of PyrPC (38 kJ/mol) is similar to that of DPPC (39 kJ/mol), the enthalpies of the mixtures are considerably lower, the minimum occurring at $X_{PyrPC} = 0.4$. This is a further indication of nonideality and closely resembles the behavior observed for mixtures of fluorodimyristoylphosphatidylcholine and dimyristoylphosphatidylcholine (Sturtevant et al., 1979).

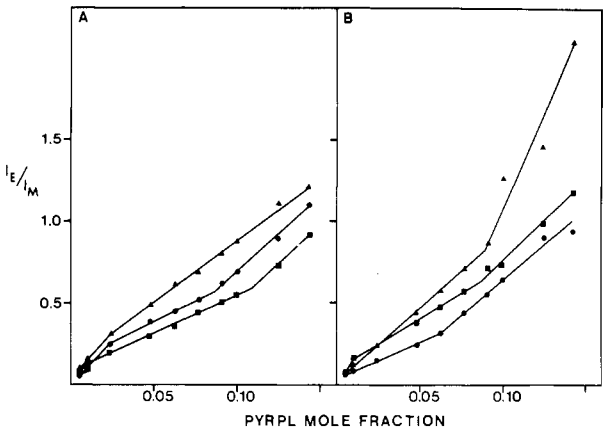

FIGURE 9: Ratio of excimer to monomer fluorescence intensities vs. X_{PyrPC} in DPPC at 25 °C. In panel A, the pyrene lipids are PyrPC (▲), PyrPG (■), and PyrPI (●) and in panel B PyrPE (▲), PyrPS (■), and PyrPA (●). For other details, see the legend to Figure 4.

Mixing of the pyrene lipids with gel-state DPPC was further investigated by measuring I_e/I_m vs. X_{PyrPC} at 25 °C. As shown by Figure 9, the plots again appear to consist of linear regions separated by kinks. This behavior indicates, in accordance with the calorimetric data, that stoichiometric aggregates are formed. However, in contrast to the situation in the liquid-crystalline state, the overall shape of the plots as well as the mole fractions corresponding to the kinks varies considerably among the pyrene lipids, indicating that head-group interactions have a marked influence on the aggregate stoichiometry. More specifically, charge repulsion may be the major factor involved since the plots for PyrPC and PyrPE run above those for the acidic pyrene lipids.

Partition of Pyrene Phospholipids between Fluid and Solid Phases. According to the concepts presented by Klausner and colleagues (Klausner et al., 1980; Klausner & Wolf, 1980), the decrease in the T_m of DPPC observed in the presence of PyrPC indicates that the pyrene lipids partition preferentially into the fluid phase. To investigate this further, DPPC liposomes containing 2.4 mol % of a pyrene phospholipid were prepared and the transition temperatures recorded both by HSDSC and by fluorometry. HSDSC scans (not shown) showed that all pyrene lipids induced, within experimental accuracy (±0.2 °C), an equal decrease of the T_m of DPPC from 41.4 to 40.7 °C, suggesting that they all prefer the fluid phase.

I_e/I_m vs. temperature scans for liposomes of identical X_{PyrPC} are depicted in Figure 10. For most pyrene lipids, the scans displayed two deflections: one around 30 °C and the second close to 40 °C. These deflections are likey to correspond to the pretransition and main transition of DPPC, respectively. The abrupt change in I_e/I_m coinciding with the main transition can be attributed to lateral redistribution of the pyrene lipid molecules (Galla & Sackmann, 1980). Above the T_m of DPPC, the probes are evenly distributed, but when the temperature is decreased and crystallization of DPPC commences, they are excluded into the remaining fluid phase. This increases the surface density of the pyrene lipids which results in increased collision frequency of the pyrene and, consequently, in increased I_e/I_m. Thus, the fluorescence data also indicate that the pyrene lipids partition preferentially into the fluid phase. All pyrene phospholipids report the main transition of DPPC at a practically identical temperature (Figure

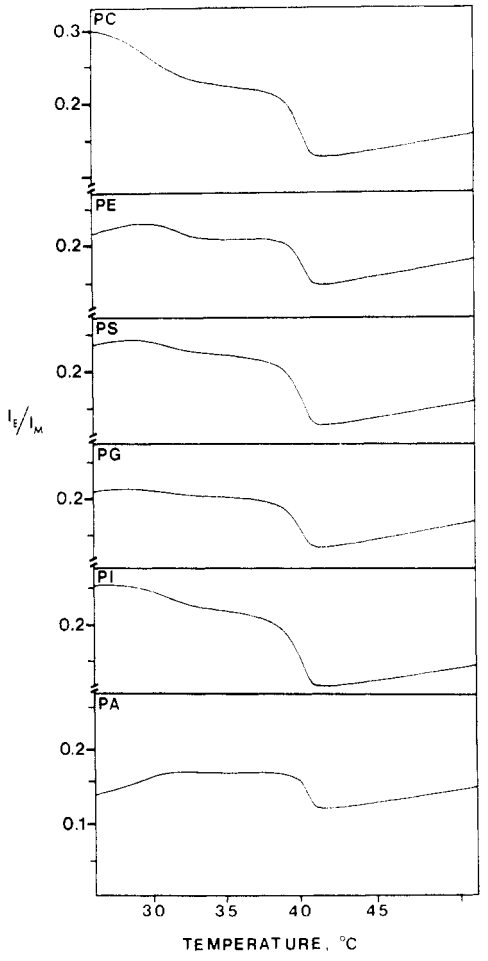

FIGURE 10: Fluorometrically detectable phase transitions in pyrene phospholipid/DPPC (2.4:97.6 mole ratio) liposomes. I_e/I_m was recorded continuously with increasing temperature as described under Materials and Methods. Total lipid concentration was 5×10^{-4} M.

10), suggesting that they all have a similar preference for the fluid phase.

Partition of parinaroylphosphatidylcholine and parinaroylphosphatidylethanolamine between coexisting fluid and solid phases has been studied recently with fluorescence polarization (Welti, 1982; Welti & Silbert, 1982). The partition behavior was found to correlate closely with the structure of the acyl chains while it was practically independent of the head group. It thus appears that partition of phospholipids between solid and fluid domains is governed by the properties of the hydrocarbon chains.

Below the T_m of DPPC, I_e/I_m is much lower for PyrPA than for the other pyrene lipids. For instance, at 25 °C, I_e/I_m for PyrPC/DPPC is more than twice that observed for PyrPA/DPPC. This could be accounted for by Coulombic repulsion which prevents clustering of PyrPA molecules to the extent possible for the neutral (zwitterionic) PyrPC.

Lateral Diffusion of Pyrene Phospholipids in Fluid EPC and DPPC Membranes. Estimates of the relative rates of diffusion of pyrene lipids can be made by comparing the slopes of the I_e/I_m vs. X_{PyrPC} plots at low X_{PyrPL} values where the excimer formation is diffusion controlled (Galla & Sackmann, 1974) and I_e/I_m thus proportional to the rate of diffusion (Table III). In DPPC, the slopes are similar for all pyrene lipids except PyrPE, for which a somewhat higher value is observed. In EPC, there is more variation; i.e., the slopes for acidic phospholipids are somewhat smaller than those for PyrPE and PyrPC. However, the difference between the highest (PyrPC) and lowest value (PyrPI) is not dramatic, and if one takes into account the probable involvement of headgroup interactions (which are expected to prohibit excimer formation with the charged pyrene lipids), it seems likely that the rate of lateral diffusion of the pyrene lipids is largely independent of the structure of the head group.

Table IV: Apparent Activation Energies for Lateral Diffusion of Pyrene Phospholipids in Liquid-Crystalline EPC and DPPC Bilayers[a]

pyrene lipid	matrix lipid	ΔE_{diff} (kJ/mol)
PyrPC	DPPC	35
	EPC	37
PyrPE	DPPC	40
	EPC	39
PyrPS	DPPC	36
	EPC	36
PyrPG	DPPC	36
	EPC	37
PyrPI	DPPC	36
	EPC	38
PyrPA	DPPC	33
	EPC	37

[a] The apparent activation energies for lateral diffusion (ΔE_{diff}) were determined as described under Materials and Methods. The temperature range was 27–42 °C in EPC and 45–55 °C in DPPC. The estimated error of ΔE_{diff} is ±5%.

The activation energies for the lateral diffusion (ΔE_{diff}) are similar for all pyrene lipids in both EPC and DPPC, the average values beeing 37 and 36 kJ/mol, respectively (Table IV). These values are in reasonable agreement with the value of 33 kJ/mol obtained previously for PyrPC in fluid phosphatidylcholine bilayers (Galla & Hartman, 1980). On the average, the values of ΔE_{diff} for PyrPE appear to be somewhat higher than those for other pyrene lipids. Whether this is due to its hydrogen bonding properties (Boggs, 1980) or to some other reasons is not known.

Taken together, these data indicate that lateral diffusion of phospholipid molecules in simple bilayers is not appreciably influenced by specific head-group interactions. Ethanolamine lipids may, however, be an exception.

Conclusions

The main purpose of the present study was to investigate the behavior of pyrene-labeled phospholipids in simple phospholipid bilayers in order to ensure proper interpretation of the data obtained with such probes from more complex systems. The results suggest that the pyrene moiety has a considerable perturbing effect on the host lipid matrix. This is indicated by the nonideal mixing of the pyrene lipids with both solid and liquid-crystalline phosphatidylcholine as well as by their preferential partition into the fluid phase. On the other hand, the pyrene moiety does not appear to modify the properties of the labeled phospholipids to the extent that a specific, head-group-mediated interaction would be masked. This is best demonstrated by the fact that the behavior or PyrPE in neat bilayers and monolayers is quite different from that of other pyrene lipids. Also, the apparent activation energy for lateral diffusion is somewhat higher for PyrPE. Finally, the individuality of the pyrene lipids is manifested in the I_e/I_m vs. X_{PyrPL} plots for pyrene lipid/DPPC mixtures at 25 °C (Figure 9), which show considerable head-group-dependent variation.

We feel that pyrene-labeled phospholipids are useful when head-group-dependent interactions between different phospholipids, phospholipids and other lipids, ions, or proteins are investigated but less so when interactions at the hydrocarbon level may be important.

ACKNOWLEDGMENTS

We are most grateful to Annikki Saulamo and Kaija Tiilikka for their secretarial assistance.

Registry No. DPPC, 63-89-8; PyrPC, 95864-17-8; PyrPE, 95864-18-9; PyrPG, 95864-19-0; PyrPI, 95864-20-3; PyrPA, 7220-34-0; PyrPS, 95891-98-8.

REFERENCES

Batzri, S., & Korn, E. D. (1973) *Biochim. Biophys. Acta 298*, 1015.

Berclaz, T., & McConnell, H. M. (1981) *Biochemistry 20*, 6635.

Boggs, J. M. (1980) *Can. J. Biochem. 58*, 755.

Chang, H., & Epand, R. M. (1983) *Biochim. Biophys. Acta 728*, 319.

Chen, S.-C., & Gaffney, B. J. (1978) *J. Magn. Reson. 29*, 341.

Chen, S.-C., Sturtevant, J. M., Conklin, K., & Gaffney, B. J. (1982) *Biochemistry 21*, 5096.

Davidson, F. M., & Long, C. (1958) *Biochem. J. 69*, 458.

Förster, Th. (1969) *Angew. Chem. 81*, 364.

Galla, H.-J., & Sackman, E. (1974) *Biochim. Biophys. Acta 339*, 103.

Galla, H.-J., & Hartman, W. (1980) *Chem. Phys. Lipids 27*, 199.

Gupta, C. M., Radhakrishnan, R., & Khorana, H. G. (1977) *Proc. Natl. Acad. Sci. U.S.A. 74*, 4315.

Hauser, H., & Dawson, R. M. C. (1967) *Eur. J. Biochem. 1*, 61.

Hauser, H., Guyer, W., & Howell, K. (1979) *Biochemistry 18*, 3285.

Hauser, H., Pascher, I., Pearson, R. H., & Sundell, S. (1981) *Biochim. Biophys. Acta 650*, 21.

Horwitz, A. F., Michaelson, D., & Klein, M. P. (1973) *Biochim. Biophys. Acta 298*, 1.

Kates, M. (1972) *Techniques in Lipidology*, pp 393–394, North-Holland Publishing Co., Amsterdam.

Klausner, R. D., & Wolf, D. E. (1980) *Biochemistry 19*, 6199.

Klausner, R. D., Kleinfeld, A. M., Hoover, R. L., & Karnovsky, M. J. (1980) *J. Biol. Chem. 255*, 1286.

Lakowicz, J. R. (1981) in *Spectroscopy in Biochemistry* (Bell, J. E., Ed.) Vol. 1, pp 195–245, CRC Press, Boca Raton, FL.

Lakowicz, J. R., Cherek, H., & Balter, A. (1981) *J. Biochem. Biophys. Methods 5*, 131.

Lenz, B., Barenholtz, Y., & Thompson, T. E. (1976) *Biochemistry 15*, 4521.

Lichtenberg, D., Petersen, N. O., Girardet, J.-L., Kainosho, M., Kroon, P. A., Seiter, C. H. A., Feigenson, G. W., & Chan, S. I. (1975) *Biochim. Biophys. Acta 382*, 10.

Mantsch, H. H., Hsi, S. C., Butler, K. W., & Cameron, D. G. (1983) *Biochim. Biophys. Acta 728*, 325.

Massey, J. B., Gotto, A. M., & Pownall, H. J. (1982) *J. Biol. Chem. 257*, 5444.

Molotkovsky, J. G., Manevich, Y. M., Gerasimova, E. N., Molotkovsky, I. M., Polessky, V. A., & Bergelson, L. D. (1982) *Eur. J. Biochem. 122*, 573.

Pagano, R. E., Longmuir, K. J., & Martin, O. C. (1983) *J. Biol. Chem. 258*, 2034.

Patton, G. M., Fasulo, J. M., & Robins, S. J. (1982) *J. Lipid Res. 23*, 190.

Petersen, N. O., & Chan, S. I. (1977) *Biochemistry 16*, 2657.

Rectenwald, D. J., & McConnel, H. M. (1981) *Biochemistry 20*, 4505.

Roseman, M., & Thompson, T. E. (1980) *Biochemistry 19*, 439.

Rouser, G., Kritchevsky, G., & Yamamoto, A. (1967) in *Lipid Chromatographic Analysis* (Marinetti, G. V., Ed.) Vol. 1, pp 99-162, Marcel Dekker, New York.

Sackmann, E. (1983) in *Biophysics* (Hoppe, W., Lohman, W., Markl, H., & Ziegel, H., Eds.) pp 425–457, Springer-Verlag, Berlin.

Shinitzky, M., Dianoux, A. C., Gitler, C., & Weber, G. (1971) *Biochemistry 10*, 2106.

Singleton, W. S., Gray, M. S., Brown, M. L., & White, J. L. (1965) *J. Am. Oil Chem. Soc. 42*, 53.

Sklar, L. A., Hudson, B. S., & Simoni, R. D. (1977) *Biochemistry 16*, 819.

Somerharju, P. J., & Wirtz, K. W. A. (1982) *Chem. Phys. Lipids 30*, 81.

Somerharju, P. J., Brockerhof, H., & Wirtz, K. W. A. (1981) *Biochim. Biophys. Acta 649*, 521.

Spencer, R. D., & Weber, G. (1970) *J. Chem. Phys. 52*, 1654.

Struck, D. K., Hoekstra, D., & Pagano, R. E. (1981) *Biochemistry 20*, 4093.

Sturtevant, J. M., Ho, C., & Reimann, A. (1979) *Proc. Natl. Acad. Sci. U.S.A. 76*, 2239.

Thuren, T., Virtanen, J. A., Vainio, P., & Kinnunen, P. K. J. (1983) *Chem. Phys. Lipids 33*, 283.

Thuren, T., Vainio, P., Virtanen, J. A., Somerharju, P. J., Blomquist, K., & Kinnunen, P. K. J. (1984) *Biochemistry 23*, 5129.

Trevelyan, W. G. (1966) *J. Lipid Res. 7*, 445.

Van Deenen, L. L. M., Houtsmuller, U. M. T., De Haas, G. H., & Mulder, E. (1962) *J. Pharm. Pharmacol. 14*, 429.

Van Dijck, P. W. M., Kaper, A. J., Oonk, H. A. J., & De Gier, J. (1977) *Biochim. Biophys. Acta 470*, 58.

Von Dreele, P. H. (1978) *Biochemistry 17*, 3939.

Welti, R. (1982) *Biochemistry 21*, 5690.

Welti, R., & Silbert, D. F. (1982) *Biochemistry 21*, 5685.

Yguerabide, J., & Foster, M. C. (1981) in *Membrane Spectroscopy* (Grell, E., Ed.) pp 199–269, Springer-Verlag, Berlin, Heidelberg, and New York.